RESEARCH ARTICLE OPEN ACCESS

OPTIMIZED SENSORLESS CONTROLTECHNIQUE WITH FLYBACK MICROINVERTER IN SOLARTILE

W.Sabitha[1], Ms.S.Abisha[2]

1 PG Student Arunachala College of Engineering for women, Manavilai, kanyakumari.

sabi05356@gmail.com

2 Assistant Professor, Arunachala College of Engineering for women, Manavilai, kanyakumari.

rajiabi194@gmail.com

----------**********----------

Abstract:

For the end user, solar energy provides a very practical and clean way to generate power. While photovoltaic (PV) panels have been the primary solar energy harvesting devices, there are several drawbacks that could cause the industry to shift toward alternative alternatives for meeting household electricity demand. PV panels are not aesthetically pleasant and come with a hefty installation cost. Due to the lack of physical sensors needed, sensorless control has the advantages of being more reliable, less expensive, and simpler to construct than sensored control. Thus, the goal of this project is to reduce the price of solar tiles by doing away with expensive current sensors. The suggested approach estimates both the high-frequency inductor current and the PV module current, removing the need for two current sensors from the standard flyback microinverter. The ripple voltage of the capacitor is used to estimate the current of the PV module. Maximum power point tracking (MPPT) and high-frequency inductor current estimation benefit from the module current estimation's capacity to adjust for fluctuations in inductance. Based on the voltage ripple that exists across the capacitor, the approach determines the PV current. To the control loop is added an inductance observer. The estimation of inductance guarantees that the control system can adjust to variations in the magnetizing inductance of the transformer. In this study, a control strategy called Grey Wolf Optimization (GWO) is used to improve the model's performance. Simulink and MATLAB 2021a are used to simulate and validate the suggested approach.

Keywords: MPPT, Solar PV module, GWO optimization, Grid and Flyback microinverter

----------**********----------

I. INTRODUCTION

Utilizing renewable energy at home is simple, and there are solutions for everyone thanks to the availability of PV cells and solar panel roof tiles. Solar tiles replace your existing roof surface, however a solar panel has roof tiles underneath it. Because solar technology is embedded into the tiles, there is less equipment visible on the top of your home. Traditional PV systems allow for easier angle adjustments, however solar panel roof tiles are fixed and only work with the existing roof's pitch. Although the technology is more compact, installing it requires a lot more work. Solar panel roof tiles have several benefits, not the least of which is their aesthetic appeal. They are also long-lasting and simple to install on listed structures. The main distinction between both is how they are put together: solar tiles are integrated into the roof's design from the beginning, replacing conventional tiling, while photovoltaic panels are added to an already-existing roof. Cables are used to link each tile to the power distribution board. Installing an inverter is required for the tiles to function properly since it turns the energy that each tile absorbs into electricity. Installing a solar diverter, also known as a "domestic solar system," is an additional option that should always be done under expert supervision. The amount of sunshine that the tiles are exposed to, which is obviously tied to the climate and the project's location, determines how much energy is generated by solar energy. Of obviously, sunny days

use less energy than foggy ones. For areas with strong sun incidence, solar tiles are a great renewable energy source. Since they are integrated into the roof design rather than added on later, they are more aesthetically pleasing and understated than conventional photovoltaic panels. Certain solar tile choices can even be completely undetectable by appearing to be ceramic or slate stone tiles. They are a fantastic choice for historic or conservation buildings that need to be renovated. Around the world, solar energy systems are gaining popularity because of their scalability and minimal emissions. On the other hand, expensive cost prevents wider use. Over time, photovoltaic (PV) systems have become more affordable. Swanson's Law, which indicates that the price of solar modules tends to reduce by 20% for every doubling of cumulative shipped volume, is widely used to anticipate the rate of decline. Consequently, it is getting harder to lower the price of solar modules. But the price of solar energy is not just determined by the cost of the modules. One method of reducing the cost of a solar installation irrespective of module cost is using building integrated PVs (BIPV). In BIPV, regular building materials are integrated with PVs. Thus, the cost of the PV installation is absorbed into the building construction cost. Solar tiles are a form of BIPV wherein rooftop shingles are integrated with solar modules. Solar energy offers a very clean and practical power generation method to the end-user. Although PV panels have been the main devices to harvest solar energy, they have some disadvantages that may divert the market to other solutions for residential electricity demand. PV panels require high installation costs and they are not visually pleasing. These issues have inspired companies to integrate solar cells into construction components. Homes are frequently surrounded by things that cast shade, such as trees, chimneys, and other dwellings. For this reason, string inverters are not a suitable choice for this use case. Since module-level optimization can prevent partial shading, DC optimizers appear to be a promising choice. Implementation presents a challenge, though, as this architecture depends on a central inverter, and maintaining a proper input voltage to the inverter requires a specific number of modules to be linked. As a result, each home would require a unique layout plan depending on the size and shape of the roof. As a result, it is not a plug-and-play solution and has higher design costs and less flexibility. For this application, PV micro-inverters appear to be the best choice.

This research suggests a cheap micro-inverter for solar tiles. A revolutionary control method that the micro-inverter uses allows it to do away with the need for current sensors in its circuitry. A PV micro-inverter typically requires two current sensors: one senses the output current to shape it into a sinusoidal waveform synchronized with the grid voltage, and the other senses the PV current for MPPT. These sensors add latency and noise to the control system, and they are expensive. This research presents a viable and economical solution for this application by doing away with the necessity for current sensors. GWO optimization algorithm is implemented in the PI controller to tune the parameters of the control system, which enhances the performance of the efficiency.

The main contribution of the research is to eliminate the current sensors from the circuit to reduce the system cost and measurement noise in the control system. To design a fly back type converter to control the solar tile micro inverter without the sensors. Usage of both the high frequency inductor current measurement as well as the photovoltaic (PV) module current measurement sensors are eliminated to reduce the system cost.

II.LITERATURE SURVEY

The unique hierarchical distributed model predictive control strategy, described by Kong et al. [1], is particularly useful for regulating stand-alone wind/solar systems. Maximum power extraction is also accounted for by the solar cell's efficiency. PV cells of the crystalline silicon variety have an efficiency of 14% to 16%. Researchers discovered that achieving an efficiency of 17–21% can be attributed to non-standard high-quality design.

According to Chen et al.'s [2] analysis of solar module efficiency by material, typical module efficiencies for copper gallium indium diselenide and cadmium telluride would be 16.4% and 17.9%,

respectively. Both the converter's switching frequency and duty cycle (D) control parameters must be changed in order to maximize power. The PV panel's low power output necessitates a certain ratio of growth. That's what the DC–DC converter will do. PV energy is used as the converter's input, and its output is an external load or attached storage supplies. Additionally, these converters will transform an unregulated DC supply into a controlled one.

For a 3ϕ PV stand-alone system, Das et al. [3] developed a new high gain converter that lessens the impact of parasitic capacitance and partial shading on the PV source. The load, power converter, MPPT control algorithm block, and solar-powered PV array make up the framework. Typically, under uniform irradiation conditions, a solar array's P–V curve has just one maximum power point (MPP), which is the point at which the PV module produces its maximum yield power.

A two-step process based on the GMPP tracking algorithm was presented by Ghasemi et al. [4]. The suggested strategy outperforms the particle swarm optimization (PSO) algorithm in PSCs in terms of tracking. Based on a natural cubic-spline-based prediction model, Huang et al. [5] presented a methodology that predicts the MPP at a much faster pace. This suggested algorithm is integrated into the iterative search procedure. The new temperature-based MPPT sensor, which is advanced in its design, is provided by Coelho et al. [6]. This technique makes use of the fact that the PV panel surface temperature directly affects the module voltage.

Bana and Saini et al. [8] used a PSO technique with binary constraints to assess the unknown parameters of the PV module's single diode model. The study that is being presented takes into consideration both monocrystalline and polycrystalline PV modules. The problem is described together with the PSO optimization, and the research gives a PV model with important mathematical modeling features. The obtained results are contrasted with the results on. The method's capacity to determine the ideality factor, parallel resistance, and series resistance simultaneously without requiring the evaluation of field information estimations is seen to make it valuable. Furthermore, the extracted parameters are calculated as a function of irradiance and temperature.

III.PROPOSED SYSTEM

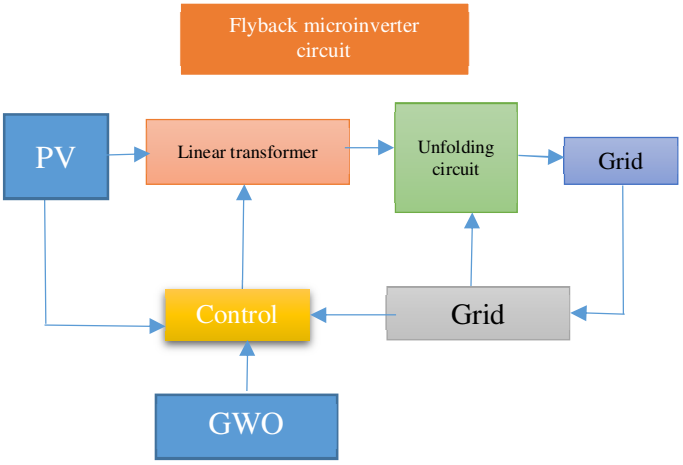

FIGURE 3.1: Proposed block diagram for a solar tile flyback microinverter with sensorless control system

The flyback converter topology serves as the foundation for the micro-inverter power circuitry in solar tile applications. Although they use a two-winding inductor, flyback converters are comparable to buck-boost converters. Higher voltage ratio capabilities and improved isolation are provided by the flyback converter. The circuit consists of an unfolding circuit at low frequency and a flyback circuit at high frequency. Both the low frequency switches at the output and the high frequency flyback switch are controlled by the control system. Grid synchronization of output current is achieved by detecting output voltage at the switching cycle frequency and adjusting the unfolding circuit and duty cycle as needed. Using the perturb and observe (P&O) approach, MPPT is carried out. Power electronic converters frequently employ one of three types of current measurement. There are several ways to remove the circuit's current measurement. For instance, the fractional open circuit voltage MPPT method uses solely the PV voltage. Generally speaking, the formula uses the open circuit voltage (Voc) to approximate the maximum power point voltage. There is one major disadvantage with this

approach, though: Efficiency is lost because the MPPT is only estimated and never fully found. Additionally, the total output power is further decreased by the intermittent module output interruption required for fractional open circuit MPPT in order to measure the open circuit voltage. For the control loop to have a high MPPT efficiency, current must be included. Because of their inexpensive cost and great power conversion versatility—they have a wide range of input and output—flyback topologies are commonly used. The flyback converter topology serves as the foundation for the micro-inverter power circuitry since cost is a major factor in solar tile applications. Although they use a two-winding inductor, flyback converters are comparable to buck-boost converters. Higher voltage ratio capacitance and improved isolation are features of the flyback converter. The circuit consists of an unfolding circuit at low frequency and a flyback circuit at high frequency. Both the low frequency switches at the output and the high frequency flyback switch are controlled by the control system. Grid synchronization of output current is achieved by detecting output voltage at the switching cycle frequency and adjusting the unfolding circuit and duty cycle as needed. Using the perturb and observe (P&O) approach, MPPT is carried out. The cost of PV micro-inverters is prohibitive when compared to alternative options. This research suggests a cheap micro-inverter for solar tiles. A revolutionary control method that the micro-inverter uses allows it to do away with the need for current sensors in its circuitry. To confirm the charging process and voltage balance, the voltages of the flying capacitors were measured at each stage. Up to a 14W power output, the voltages were measured at each 50mA increment. The voltage across the flying capacitors maintains between one-third and two-thirds of the output voltage at each point. For instance, the voltages for C1, C2, and Cout are 20V, 40V, and 60V, respectively, at the 9Wpoint. In this instance, C1, which is closer to the secondary coil than the flyback converter, preserves the primary reflected voltage, which is reduced to one-third of the output voltage. While steady-state performance is being compared to dynamic performance, load step-response is not displayed but is anticipated to be comparable to other multilevel converters.

3.1 CURRENT ESTIMATER:

The ripple voltage of the capacitor is used to estimate the current of the PV module. Maximum power point tracking (MPPT) and high-frequency inductor current estimation benefit from the module current estimation's capacity to adjust for fluctuations in inductance. The PV voltage and duty cycle inputs are used by the current estimator block to calculate the instantaneous inductor current value. PV current is also calculated in order to feed it into the MPPT block. To perform this computation, one need only take the inductor current and average it across time. A PI controller is used to drive PV voltage to the desired reference voltage. The MPPT block employs the P&O method to determine a reference voltage from input PV voltage and estimated PV current.

3.2 INDUCTANCE OBSERVER:

An inductance observer can be used to react to various inductance values when the CCM process is initiated. By comparing the outcomes of two current calculations, the observer adjusts the inductance value in the control system to determine the inductor current. An inductance observer can generate the required inductance value and respond to changes in it in an adaptive manner. When exposed to varying inductance values, the high frequency inductor current maintains accuracy because the inductance can be approximated.

3.3P&Oalgorithm:

Every test was conducted using the perturb and observe (P&O) technique. P&O is a well-liked MPPT algorithm that's frequently used to measure other MPPT algorithms against. In P&O, the initial stage is to cause a disturbance to Power is calculated by multiplying the voltage and current measurements taken over a period of time following the disturbance. The power computed in the current time interval is contrasted with the power computed in the preceding time interval. The same perturbation is carried out again if the power is increased, and the opposite perturbation is carried out if the power is decreased. Both the duty cycle step modification and the iteration period were maintained constant throughout the testing to ensure uniformity. A PI

controller is used to drive PV voltage to the desired reference voltage. The MPPT block employs the P&O method to determine a reference voltage from input PV voltage and estimated PV current.

3.4 MPPT:

A PV system should contain an efficient maximum power point tracking (MPPT) controller in addition to an efficient inverter that is also reasonably priced. Any of the listed algorithms, except perturb and observe, could be used to obtain the MPPT in the majority of PV systems. PV voltage and current must be measured in order to apply any of the aforementioned MPPT techniques. Appropriate corrective action, such as adjusting the duty ratio or reference magnitude, must then be done in order to maximize the power output from the PV panel or module. The grid-interactive PV micro-inverter primarily supports reactive power and has a bidirectional boost-buck DC-DC converter with a high step-up ratio. Using constant voltage as the MPPT approach, a PV current sensor-free dual stage flyback grid-connected inverter structure.

3.5 DIGITAL TO ANALOG CONVERTER:

A digital to analog converter (DAC) receives a reference peak current from the digital control system. The Reset signals for a Set-Reset latch, which provides the switching signals to a gate driver, are produced by the DAC feeding into an analog comparator. This ensures that the converter will never enter CCM and become unstable and allows for control over the peak current.

3.6 PI CONTROLLER:

When the calculated current reaches the specified magnitude, the gate pulses stop. The immediate rectified grid voltage and the proportional integral (PI) controller output define this magnitude. PV voltage is driven to the required reference voltage using a PI controller.

3.7 CURRENT SENSORLESS SYSTEM:

A two-stage flyback PV current sensorless system to lower both the price and the system's footprint. On the other hand, a number of academics have put forth a number of methods to deal with a PV module's maximum power point tracking (MPPT) mechanism without having to measure its PV current. This is relevant to practice since these methods allow for the removal of the DC-current sensor, making a system more financially viable to install. Grid-interactive PV micro-inverters have focused on and explored PV current sensor-less or MPPT-free approaches. This work uses P&O MPPT technique to explain two stages with high boost ratio without using PV-current sensor. As a result, using the PV voltage and its predicted current, which is obtained from the ac-grid current, the optimal power is calculated.

3.8 MICRO INVERTERS:

A variety of microinverters for photovoltaic modules are on the market. Nonetheless, it is evident that isolated systems which are typically employed increase the system's size, weight, and expense. A frequent setup that lowers efficiency and lifespan is several stage inverters. At their highest power, commercially available microinverters have an efficiency that ranges from 85% to 95%. One more method is to use single-stage transformerless microinverters, which have an extremely efficient architecture. This topology's primary flaw is the hard switching of high-frequency switches, which results in large switching losses and issues with electromagnetic interference. The Boost microinverter, as detailed in, was intended specifically as a rooftop solar PV system microinverter. However, the topology was unsuitable for BIPV applications since it used large inductors. The inverter shown here increases the voltage by utilizing the concept of a charge-pump model based on a capacitor circuit. To stop leakage current, it is double grounded. However, because of the non-symmetric input current, controlling its Maximum Power Point Tracking (MPPT) is challenging.

3.9 VOLTAGE SENSORLESS MPPT:

To replace PV voltage, the suggested MPPT technique requires an electric charge quantity. The PV current and the off-time are used to calculate the amount of electric charge. Thus, the PV current and electric charge amount determine the maximum power. PV current is measured in order to determine the maximum power. For P&O MPPT, the current perturbation is computed after the PV power has been determined. To determine which way to apply the perturbation, consider the signs of P and I. Phase locked loops (PLLs), which produce in-phase sinusoids, are utilized to create the rectified

waveform synchronized grid voltage. When operating in the grid-connected mode, a quick and precise PLL mechanism is since it is the foundation of the current reference. PWM signal generated by a line frequency PWM generator using the PLL output signal controls the switches SS-1 and SS-2. The PLL output signal is used to determine the absolute sin generator's resultant signal. The PV current and electric charge amount, which are determined using the PV current and the power calculator's resultant signal, are used to compute the current reference producer for the reference current. The output signal sent to a PI controller calculates the off-time calculator's resultant signal. The PV current and current reference producer are used to determine the PI controller's resultant signal in relation to the current reference signal. The absolute sin generator's resultant signal is used to calculate the output reference current, or i*out.

3.10 GWO OPTIMIZATION:

The hunting strategy and leadership structure of grey wolves are modeled by the GWO algorithm. Alpha, beta, delta, and omega are the four varieties of grey wolves that are used to model the leadership hierarchy. Furthermore, in order to carry out optimization, three primary phases are used: hunting, looking for prey, encircling prey, and attacking prey.

Inspiration:

Grey wolf belongs to Canidae family. Grey wolves are considered as apex predators, meaning that they are at the top of the food chain. Grey wolves mostly prefer to live in a pack. The group size is 5-12 on average. Of particular interest is that they have a very strict social dominant hierarchy. The alphas, a male and a female pair, are the leaders. The alpha is mostly in charge of choosing where to hunt, where to sleep, when to wake up, and other decisions. The pack is subject to the alpha's judgments. But there has also been evidence of a democratic tendency, when an alpha wolf follows the other wolves in the pack. When the pack is together, all of the members bow down to the leader. Because the pack should obey the commands of the alpha wolf, this wolf is sometimes referred to as the dominating wolf. Only within the pack are the alpha wolves permitted to mate. It's interesting to note that the alpha is the best pack manager rather than the strongest member. Beta is the second rung on the grey wolf hierarchy. When it comes to making decisions or helping the alpha with other pack tasks, the betas are subordinate wolves. The beta wolf, who can be either male or female, is most likely the most qualified candidate to become the alpha in the event that one of the alphas dies or grows very old. Although the beta wolf commands the other lower-level wolves as well, it should nevertheless show respect to the alpha. It serves as the pack's disciplinarian and advisor to the alpha. Throughout the pack, the beta confirms the alpha's orders and provides the alpha with feedback. Omega is the lowest ranking grey wolf. The omega acts as the victim of blame. Omega wolves must always yield to All other dominant wolves must always yield to omega wolves. These are the final wolves permitted to consume food. Although the omega may not appear like a significant member of the pack, it has been noted that when the omega is lost, the pack as a whole has internal conflict and issues. This is because the omega(s) let loose with their aggression and their displeasure with all the wolves. This helps to preserve the dominance structure and satiate the needs of the entire pack. The pack's babysitters might also be the omega in certain situations.

Encircling prey:

Grey wolves encircle their victim when they are hunting. To represent encircling behavior analytically. The position of the prey (X*,Y*) can be used by the grey wolf in position (X,Y) to update its own position. By changing the vector values, it is possible to reach several locations around the optimal agent in relation to the current position.

Hunting:

Grey wolves are able to locate their prey and circle around them. The alpha typically leads the hunt. Every now and then the beta and delta may also go hunting. However, we are clueless as to where the optimal (prey) is located in an abstract search space. We assume that the alpha (best candidate solution), beta, and delta have superior knowledge regarding the possible location of prey in order to mathematically recreate the hunting behavior of grey wolves. As a result, we reserve the top three results thus far and require the other search agents—

including the omegas—to adjust their positions in accordance with the best search agent's position. Furthermore, the ultimate position would be at random inside a circle that is determined by the search space's coordinates for alpha, beta, and delta. Stated differently, other wolves update their positions randomly around the prey, whereas alpha, beta, and delta estimate the prey's position.

Exploitation phase:

After their hunt is over, grey wolves attack their victim when it stops moving. By using the operators that have been suggested thus far, the GWO algorithm enables its search agents to attack the prey by updating their position in relation to the alpha, beta, and delta's locations. With these operators, the GWO algorithm is prone to stalling in local solutions. While the proposed encircling mechanism does demonstrate some exploration, GWO still requires more operators to prioritize exploration.

Exploration phase:

Grey wolves primarily use the alpha, beta, and delta positions to guide their searches. They split off to find prey and then come together to attack it. We use with random values higher than 1 or less than -1 to force the search agent to diverge from the prey in order to mathematically simulate divergence. Exploration is prioritized, and the global search capability of the GWO algorithm is enabled. In an attempt to locate a better meal, the grey wolves are forced to stray from their prey when |A|>1. Another element of GWO with random values in [0, 2] that encourages investigation. In order to stochastically accentuate (C>1) or de-emphasis (C<1) the role of prey in defining the distance in Equation (3.1), this component offers random weights for prey. In summary, the GWO algorithm generates a random population of grey wolves (candidate solutions) at the beginning of the search process. Alpha, beta, and delta wolves then assess the likely position of the prey through a series of iterations, with each candidate solution updating its distance from the prey.

Initialize the grey wolf population Xi(i=1,2,….n)

Initialize a, A, and C

Calculate the fitness of each search agent

X_a **=the best search agent**

X_β **=the second best search agent**

X_δ **=the third best search agent**

while (t **< Max number of iterations)**

for each search agent

Update the position of the current search agent by above equations

end for

Update α, A *and* C

Calculate the fitness of all search agents

Update X_α, X_β *and* X_δ

t=t+1

end while

Return X_α

Psuedocode for GWO optimization

4. RESULTS AND DISCUSSIONS:

MATLAB is used as a implementation platform to obtain the efficient performance results, which provides the efficient results and compared with the other techniques to enhance the model efficacy.

4.1 SIMULATION DIAGRAM

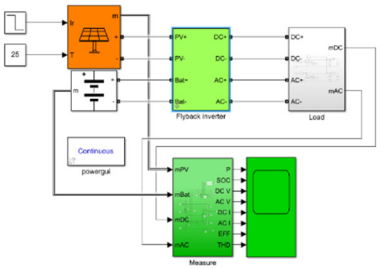

FIGURE 4.1: Overall Simulation diagram

PowerSIM is used in this section to model the flyback microinverter. The methods for estimating current and inductance are validated using circuit and control system simulation. An ac power source is supplied to the simulated grid by the flyback microinverter, which receives dc power from a replicated solar module. Properties of the physical solar tile, for which the circuit was developed, were modeled in order to emulate the solar module.

Figure 4.3 Optimized PI controller simulink diagram

4.2 PARAMETER SPECIFICATIONS OF THE SIMULINK DIAGRAM:

Sl.no	PARAMETERS		RANGE
1.	Solar PV array	Maximum power	392.32 W
		Short-circuit current	9.39
		Voltage at maximum power point	44
		Current at maximum power point	9.03
2.	Boost converter	IGBT Resistance	0.001
3.	PI Controller	Reference voltage	250 V
		Kp gain	0.0005
		Ki gain	0.04

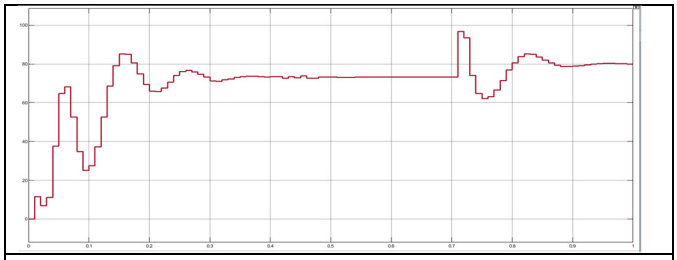

Efficiency

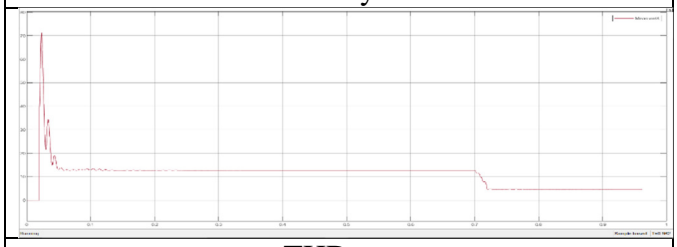

THD

Figure 4.4: Output waveform of efficiency and THD

PowerFlow in the Solar pv which represents the powerflow of DC power, AC power, Power loss, Battery power and PV power.Corresponding results are outperformd while absorption and generation. Output of AC voltage which attains at a maximum voltage at 300V. The output of AC current which increases from 0.7 to 3.8. Output waveform of DC current which depends upon the Irradiance level of Solar PV. Efficiency Output increases the ranges from 70 to80%. The output waveform of SOC curve which depends upon the rate of power flow.

5. CONCLUSION:

A brand-new PV microinverter control system without a current sensor was created and put to the test. MPPT can be effectively executed by the flyback converter without the requirement for current measurement. Additionally, by adjusting for the various inductance values, the suggested state observer can guarantee an accurate estimation for high frequency current. The MPPT efficiency of the new control system was compared to control systems that have been published in the past as well as a control system that has sensors in order to show performance. Compared to other sensorless systems available now and reported in earlier research, the innovative method's MPPT efficiency was noticeably greater. The suggested method's MPPT efficiency is comparable to the sensor-equipped MPPT's. It should be observed that the system experiences poorer efficiency and has trouble functioning at low power due to the additional control complexity of the inductance estimation. Consequently, it is not advised to use the inductance estimate at low power. It is also unnecessary, though, as changes in inductance won't result in low current entrance into CCM mode operating. The GWO algorithm optimizes the control system, improving the sensor-less control system's output performance. As a result, the control system can continue to function well even without the requirement for current measurement. Eliminating the current measurement lowers the cost of the circuit's components, cuts down on circuit losses, and lowers the control system current's signal to noise ratio. The elimination of the current measurement reduces the component cost of the circuit, decreases losses in the circuit, and reduces the signal to noise ratio of the control system current. By this proposed optimization, 88.2% efficiency is obtained from the control system and the Total Harmonic Distortion

(THD) rate is reduced by optimizing the control parameters in the system.

ACKNOWLEDGEMENT:

The authors would like to thank Arunachala College of Engineering for supporting this research.

6. REFERENCES:

1. Falconer, Nicholas, Dawood Shekari Beyragh, and Majid Pahlevani. "An adaptive sensorless control technique for a flyback-type solar tile microinverter." IEEE Transactions on Power Electronics 35, no. 12 (2020): 13554-13562.
2. G. K. Singh, Solar power generation by PV (photovoltaic) technology: A review, Energy, vol. 53, pp. 113, May. 2013.
3. D. Muoio, Tesla has said little about its solar roof since it began taking orders here's what we do know, Internet: http://www.businessinsider.com/tesla-solar-roof-details-features-pictures-2017-8/, Aug. 4, 2017 [Nov. 21,2017]
4. A. M¨aki and S. Valkealahti, Power losses in log string and parallel connected short strings of series-connected silicon-based photovoltaic modules due to partial shading conditions, IEEE Trans. Energy Convers., vol. 27, no. 1, pp. 173-183. Mar. 2012.
5. N. D. Kaushinka and A. K. Rai, An investigation of mismatch losses in solar photovoltaic cell networks, Energy vol. 32, no. 5, pp. 755-759. May 2007
6. R. C. N. Pilawa-Podgurski and D. J. Perreault, Submodule integrated distributed maximum power point tracking for solar photovoltaic applications, IEEE Trans. Power Electron. vol. 28, no. 6, pp. 29572967, Jun.2013.
7. N. Sukesh, M. Pahlevaninezhad and P. K. Jain, An investigation of mismatch losses in solar photovoltaic cell networks, IEEE Transaction son Industrial Electronics, vol. 61, no. 4, pp. 1819-1833, Apr. 2014.
8. T. Shimizu, K. Wada, and N. Nakamura, Flyback-Type Single-Phase Utility Interactive Inverter With Power Pulsation Decoupling on the DC Input for an AC Photovoltaic Module System, IEEE Trans Power Electron, vol. 21, no. 5, pp. 1264 - 1272, Sept. 2006.
9. T. Shimizu, K. Wada, and N. Nakamura, A flyback-type single phase utility interactive inverter with low-frequency ripple current reduction on the DC input for an AC photovoltaic module system, in Proc. IEEE PESC, 2002, pp. 1483-1488.
10. N. Kasa, T. Iida, and L. Chen, Flyback inverter controlled by sensorless current MPPT for photovoltaic power system, IEEE Trans. Ind. Electron., vol. 52, no. 4, pp. 11451152, Aug. 2005.
11. M. A. Rezaei, K. J. Lee and A. Q. Huang. A High-Efficiency Flyback Micro-inverter With a New Adaptive Snubber for Photovoltaic Applications, IEEE Trans. on Power Electron., vol. 31, no. 1, pp. 318-327,Jan. 2016.
12. M. Pahlevani, S. Eren, J. M. Guerrero and P. Jain, A Hybrid Estimator for Active/Reactive Power Control of Single-Phase Distributed Generation Systems With Energy Storage, in IEEE Transactions on Power Electronics, vol. 31, no. 4, pp. 2919-2936, April 2016.
13. S. Eren, M. Pahlevaninezhad, A. Bakhshai and P. K. Jain, Composite Nonlinear Feedback Control and Stability Analysis of a Grid-Connected Voltage Source Inverter With LCL Filter, in IEEE Transactions on Industrial Electronics, vol. 60, no. 11, pp. 5059-5074, Nov. 2013.
14. R. Hermann and A. Krener. Nonlinear controllability and observability, IEEE Transactions on Automatic Control, vol. 22, no. 5, pp. 728-740 Oct. 1977
15. M. Pahlevaninezhad, S. Eren, H. Pahlevani, I. Askarian and S. Bagawade. Digital Current Sensorless Control of Current-Driven Full-Bridge DC/DC Converters, IEEE Trans. on Power Electron., vol. 33, no.2, pp.1797-1815, Mar. 2017
16. S. Diop and M. Wang, Equivalence between algebraic observability and local generic observability, Proc. 32nd IEEE Conf. on Decis. Control,1993 pp. 2864-2865.
17.I. Askarian, S. Eren, M. Pahlevani and A. Knight, Digital Real-Time Harmonic Estimator

for Power Converters in Future Micro-Grids, IEEE Transactions on Smart Grid, June 2017.

18. M. Pahlevani, S. Pan, S. Eren, A. Bakhshai and P. Jain, An Adaptive Nonlinear Current Observer for Boost PFC AC/DC Converters, in IEEE Transactions on Industrial Electronics, vol. 61, no. 12, pp. 6720-6729, Dec. 2014.
19. S. Eren, M. Pahlevani, A. Bakhshai and P. Jain, A Digital Current Control Technique for Grid-Connected AC/DC Converters Used for Energy Storage Systems, in IEEE Transactions on Power Electronics, vol. 32, no. 5, pp. 3970-3988, May 2017.380

